



# Generation of Artificial Acoustic-Gravity Waves and Traveling Ionospheric Disturbances in HF Heating Experiments

R. Pradipta · M. C. Lee · J. A. Cohen · B. J. Watkins

Received: 30 June 2014 / Accepted: 28 January 2015 / Published online: 7 February 2015  
© Springer Science+Business Media Dordrecht 2015

**Abstract** We report the results of our ionospheric HF heating experiments to generate artificial acoustic-gravity waves (AGW) and traveling ionospheric disturbances (TID), which were conducted at the High-frequency Active Auroral Research Program facility in Gakona, Alaska. Based on the data from UHF radar, GPS total electron content, and ionosonde measurements, we found that artificial AGW/TID can be generated in ionospheric modification experiments by sinusoidally modulating the power envelope of the transmitted O-mode HF heater waves. In this case, the modulation frequency needs to be set below the characteristic Brunt–Vaisala frequency at the relevant altitudes. We avoided potential contamination from naturally-occurring AGW/TID of auroral origin by conducting the experiments during geomagnetically quiet time period. We determine that these artificial AGW/TID propagate away from the edge of the heated region with a horizontal speed of approximately 160 m/s.

**Keywords** Artificial acoustic gravity waves · Traveling ionospheric disturbances · HF ionospheric heating · Total electron content · Ionosonde sky maps

## 1 Introduction

For 5 years or so (2008–2012), we have conducted a series of ionospheric HF heating experiments in Gakona, Alaska to generate artificial acoustic-gravity waves (AGW) that

---

R. Pradipta (✉)  
Institute for Scientific Research, Boston College, Newton, MA 02459, USA  
e-mail: rezy.pradipta@bc.edu

R. Pradipta · M. C. Lee · J. A. Cohen  
Space Propulsion Lab, Massachusetts Institute of Technology, Cambridge, MA 02139, USA

M. C. Lee  
Department of Electrical and Computer Engineering, Boston University, Boston, MA 02215, USA

B. J. Watkins  
Geophysical Institute, University of Alaska Fairbanks, Fairbanks, AK 99775, USA

are detectable by several radio diagnostic instruments as traveling ionospheric disturbances (TID) (Pradipta 2012). The experiment provides positive evidence that large-scale thermal gradients could act as a source of free energy to produce AGWs in the atmosphere. This finding corroborates a proposed natural scenario (Pradipta 2007) in which large-scale thermal fronts associated with severe heat wave events generate AGWs that can reach the upper atmosphere and subsequently trigger intense TIDs over extensive areas.

Effective heating of ionospheric plasmas using HF heater in continuous wave O-mode can yield a depleted magnetic flux tube, due to thermal expansion as well as chemical reactions caused by the heated ions (Lee et al. 1998). Thus, we may expect that the temperature of neutrals inside the heated region can be increased to form significant thermal gradients. The possibility for such heater-induced temperature gradients to generate AGWs had been remarked by Luhmann (1983). Previously, a theoretical investigation on the process of AGW generation by high-power HF radio transmitters had also been presented by Grigor'ev (1975). In the meantime, based on the dynasonde ionogram data recorded at the Platteville research facility, there had been some indication of AGW/TID being observed during ionospheric heating experiments (NOAA documentation 2004; Wright 1975) but very little attempt was made to conclusively determine whether these disturbances were heater-induced artificial AGWs or natural AGWs from elsewhere. In general, there was a lack of definitive answer regarding the generation of artificial AGWs from the early ionospheric heating experiments. However, more recent development (Mishin et al. 2012; Kunitsyn 2012) from a number of independent experimental investigations concurrent with ours have provided some new and useful insight on this question. Finally, the results from our ionospheric heating experiments (reported here) also offer consistent evidence that further confirms the ability of heater-induced thermal gradients to generate artificial AGW/TID.

This paper begins with a brief description of the heating scheme and the setup of diagnostic instruments that we used in the experiments. We address the rationale behind the heating modulation scheme to generate AGWs, as well as the fundamental strategy on the usage of each radio diagnostic instruments. Experimental results based on the data collected by these diagnostic instruments (UHF radar, digisonde, GPS) are discussed in three separate subsections. Following the data discussion, a few additional remarks and the conclusion of current work are presented at the end of this paper.

## 2 Experimental Setup

In our experiments, we generated artificial AGW/TID by inducing time-varying thermal gradients directly at ionospheric height via a modulated HF heating scheme. The basic purpose of this experiment is to physically simulate the plausible scenario of AGW generation by anomalous large-scale natural thermal fronts (e.g. severe heat wave events), which might subsequently trigger widespread plasma turbulence in the ionosphere in the form of TID. The experiments were carried out at the High-frequency Active Auroral Research Program (HAARP) facility located at geographic coordinate 62.4°N and 145.1°W, at Gakona, Alaska. In total, there were 17 separate runs of the HAARP-AGW experiment over 5 years (2008–2012).

To generate artificial AGW/TID in our HAARP-AGW experiments, we used the high-power HF antenna array at the HAARP facility to transmit O-mode HF heater waves vertically into the ionosphere. The heater wave frequency  $f_{\text{HF}}$  was set to be below the peak ionospheric plasma frequency ( $f_{\text{oF2}}$ ), and the interaction region is typically located at an

altitude of 200–250 km above the earth’s surface. Furthermore, the HF heater wave was amplitude-modulated so that the level (i.e. the envelope) of transmitted power would vary sinusoidally with time (starting at zero power, and the power modulation frequency shall be denoted by  $\Omega$ ). This sinusoidal power modulation controlled the rate of energy deposition into the heated plasma volume, thus creating thermal gradients that vary with time as  $\sim \exp(i\Omega t)$ . As a result of this modulated heating, AGW/TID would be radiated outward from the heated plasma region.

To ensure that we were generating the (internal) gravity wave branch and not the acoustic wave branch, we had to set the modulation frequency to be lower than the local Brunt–Vaisala frequency  $\omega_g$  within the interaction region. In the altitude range of 200–250 km, we estimated (using the NRL MSIS-E atmospheric model) that the Brunt–Vaisala period is approximately  $2\pi/\omega_g = 10\text{--}11$  min. Based on this estimate, a modulation period of  $2\pi/\Omega = 12$  min had been selected for this heating experiment. In addition to satisfying the condition  $\Omega < \omega_g$  that we specified earlier, a 12-min modulation period would also make a whole integer number of modulation cycles that fit adequately in a full-hour schedule block.

Figure 1 illustrates the basic setup of the HAARP-AGW experiment, depicting the HF heater beam together with the configuration of several radio diagnostic instruments. During the experiments, these instruments monitored the ionospheric plasma condition inside and around the heated volume. First of all, the Modular UHF Ionospheric Radar (MUIR) was

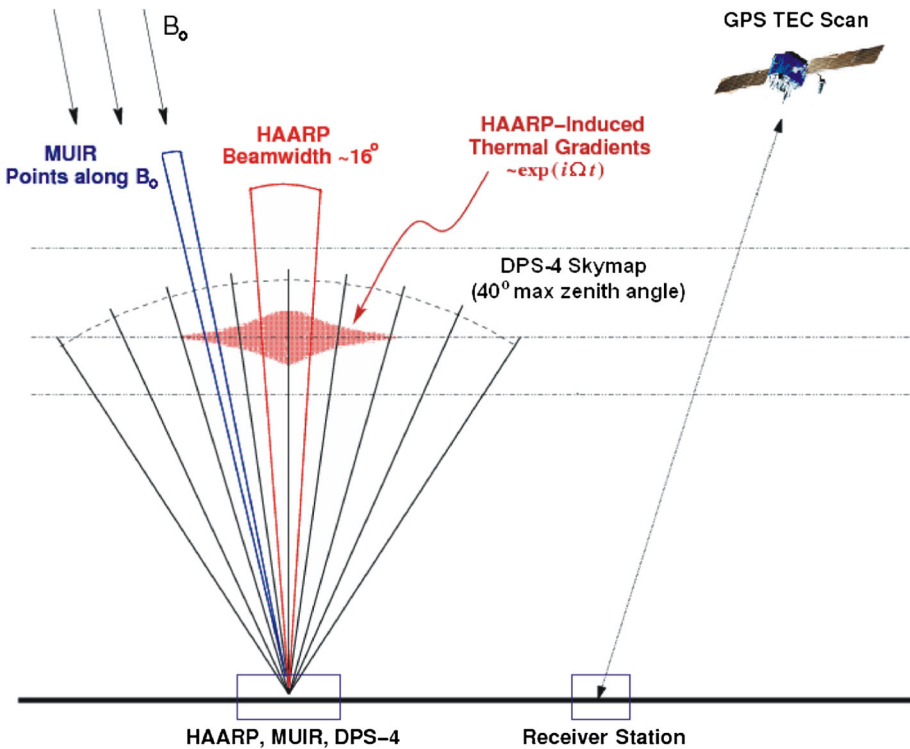


**Fig. 1** Basic experimental setup for the HAARP-AGW experiments. We used a number of satellite and ground-based radio diagnostic instruments to detect the heater-generated artificial AGW/TID

configured to point along the geomagnetic field lines, roughly at an angle of  $15^\circ$  from vertical. Here we used MUIR as a collective Thomson scatter diagnostics to measure the line-of-sight (LOS) plasma velocity outside the heated plasma volume. Meanwhile, the on-site digisonde at the HAARP facility was set to record skymaps throughout the experiments—in addition to one regular ionogram measurement every 5 min. We mainly looked at the spatial pattern of return echoes in the skymap data to identify and track the artificial traveling plasma disturbances that emanated from the heated region during our experiments. Finally, we also measured the total electron content (TEC) from GPS satellite passes near the HAARP facility around the time period of our experiments. In this case, we examined the TEC perturbation (TECP) signal to look for the characteristic signatures of the artificial AGW/TID that resulted from the modulated HF heating.

Using these multi-diagnostic radio measurements, we shall demonstrate that artificial AGW/TID had been generated during our experiments. More specifically, we need to show that the observed traveling plasma disturbances in fact originated from the heated region (not naturally-occurring ones that happen to pass by) and exhibited key characteristics matching those of the heating modulation pattern (e.g. in terms of their periodicity). In relation to the abovementioned requirements, note also that we had carried out the HAARP-AGW experiments during quiet geomagnetic condition to avoid possible contamination from AGW/TID of auroral origin.

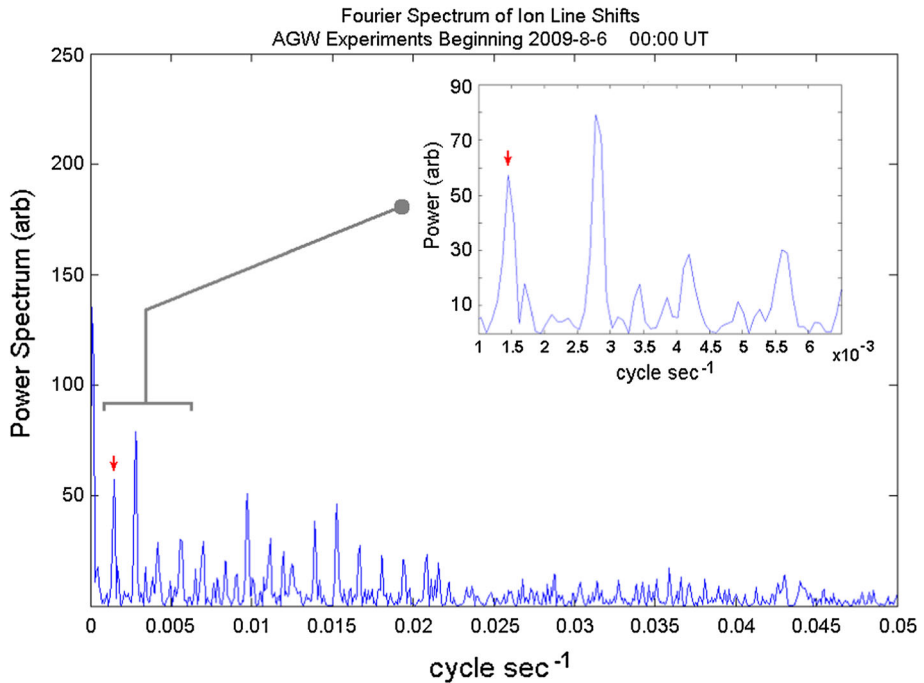
### 3 Experimental Results

In this section, we discuss several findings based on the data recorded during the HAARP-AGW experiments. From both ground-based and satellite diagnostic data, we have obtained several positive indications that AGW/TID had emanated from the heated plasma volume, generated as a result of the modulated HF heating performed during our experiments. Presented here are the data from MUIR radar, digisonde, and GPS satellite measurements.

#### 3.1 MUIR Radar Observations

During the HAARP-AGW experiments, the 446 MHz MUIR diagnostic radar was set to point at an angle of  $15^\circ$  from vertical—along the background geomagnetic field line. By aiming the radar beam well-outside the heated plasma volume, we would have intercepted the artificial traveling plasma disturbances as they propagated radially away from the heated region. The MUIR radar was configured to record ion-acoustic lines from the ionospheric F-region, and we have been able to infer the LOS velocity based on the Doppler shift of the ion-acoustic line. The wind velocity fluctuation associated with the generated artificial AGW/TID would then give rise to periodic time variation in the MUIR LOS velocity, with the same periodicity as that of the heating modulation cycle.

Using the return signals from the 170–320 km range, we computed the MUIR ion line spectra. Since the ion line spectra inferred from individual radar pulses are noisy, we have integrated the spectra over 500 pulses to obtain clearer ion line spectra. Next, we used each one of the integrated ion line spectra to determine the centroid of the ion-acoustic line, and then took these centroid values to compile a time series of the Doppler shift. The Doppler shift time series is equivalent to the LOS velocity as a function of time, and we shall look for a periodic time variation in this time series that would indicate that some AGW/TID (with 12-min period) had been intercepted by the MUIR radar beam.



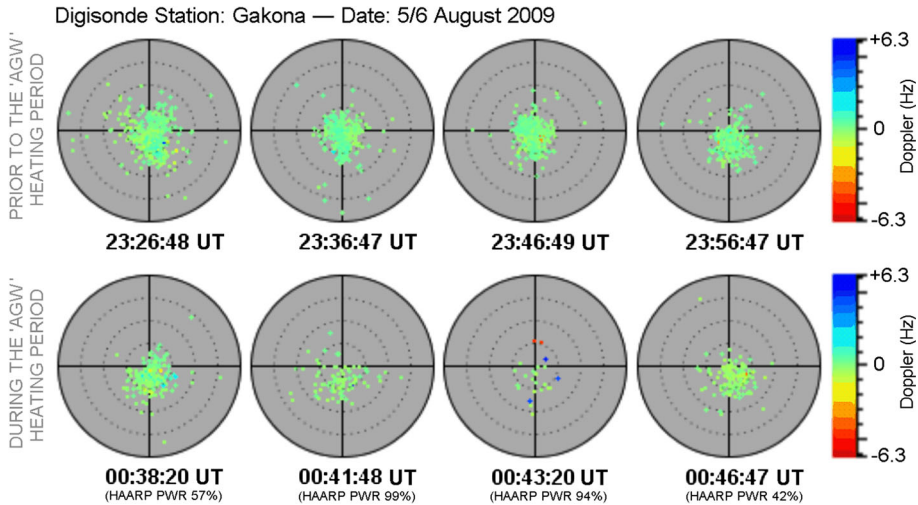
**Fig. 2** Fourier periodogram of the Doppler shift time series derived from the MUIR ion-acoustic lines recorded during the HAARP-AGW experiment on 6 August 2009 00:00-02:10 UTC

Figure 2 shows a Fourier periodogram of the Doppler shift time series derived from MUIR ion line data that were recorded during the HAARP-AGW experiment conducted on 6 August 2009 00:00-02:10 UTC. One may notice a prominent peak at approximately 1.4 mHz along with some of its harmonics up to 20 mHz or so. In our experiments, we had modulated the transmitted HF power sinusoidally with a period of 12 min, which corresponds to a frequency of 1.39 mHz. Thus, the prominent peak at  $\sim 1.4$  mHz reveals a periodic time variation with a periodicity that is very close to 12 min. Meanwhile, the presence of some harmonics tells us that the observed periodic time variation was not perfectly sinusoidal.

This result in general indicates that we have observed a wind speed fluctuation pattern (outside the heated region) that varied periodically with time when we were modulating the transmitted HF heater power. The periodicity of the aforementioned wind speed variation closely matches the 12-min power modulation period, suggesting that some artificial AGW/TID had been generated and subsequently intercepted by the MUIR radar beam. Some skymap data that had been recorded during this particular run of the HAARP-AGW experiment are also presented and discussed in the next subsection.

### 3.2 Digisonde Skymap Data

Skymap measurements using the digisonde (i.e. digital ionosonde) provide useful Doppler shift and directionality information on the return echoes that are captured by the receiving antennas. The spatial gradation of the Doppler shift pattern can be used to infer the



**Fig. 3** A set of digisonde skymap data recorded on 5/6 August 2009, showing broad sequential snapshots of the F-region ionosphere prior to the HAARP-AGW experiment (*top row*) and a series of consecutive higher-cadence skymaps taken during the HAARP-AGW heating period (*bottom row*)

background  $\mathbf{E} \times \mathbf{B}$  plasma drift velocity. A complete directionality information (i.e. virtual range and zenith/azimuth arrival angles) on the return echoes also allows us to map the virtual echolocation in 3-D coordinate space. By monitoring how the spatial distribution of the virtual echolocations changes with time, we have been able to detect the artificial traveling plasma disturbances that propagated away from the heated region during our experiments.

Figure 3 shows some sample skymaps relevant to the HAARP-AGW experiment conducted on 6 August 2009 00:00–02:10 UTC. Prior to the experiment, skymaps were recorded at a rate of one skymap every 5 min. As the HAARP-AGW experiment started, skymaps were recorded at a higher rate of one skymap every 1–2 min. The top row of Fig. 3 consists of several skymaps sampled before the HAARP-AGW heating started, which show a relatively uniform and constant spatial distribution of return echoes from ionospheric F-region plasma. This pattern was consistently observed over an extended period of time until the HAARP-AGW experiment started at 00:00 UTC. Meanwhile, the bottom row of Fig. 3 depicts a series of consecutive skymaps recorded during the HAARP-AGW heating period. These skymaps show how the spatial distribution of return echoes changed over time as a HAARP-AGW heating cycle progressed.

We also indicate the instantaneous level of the transmitted HF heater power underneath each one of these skymaps (at 00:42 UTC, a power maximum occurred). The overall amount of return echoes in the skymaps was found to dip/decrease substantially as the HAARP-AGW heating cycle passed around a maximum. However, we should also note that it occurred with certain time delay: in this case the transmitted HF heater power reached a maximum at 00:42 UTC, but the most severe reduction in the skymap echoes during this cycle actually happened at 00:43:20 UTC (HAARP power had gone down from 99 % to 94 %). This time delay indicates that the aforementioned skymap echo reduction was not dominated by the effects of HF-induced ionospheric irregularities, which would manifest themselves with virtually no delay (given the high level of transmitted HAARP power that reached 3.6 MW at its maximum). Rather, the observed reduction in skymap

echoes during this experiment must have been primarily controlled by dynamical process(es) involving the inertia of plasma and neutral fluids around the heated plasma volume. These physical characteristics would be consistent with the generation of AGW as a result of the modulated heating cycle. The loss of skymap echoes in this case can be attributed to multiple refractive deflections of the digisonde's radio diagnostic rays by the AGW-disturbed isoionic surfaces, both below and above the heated plasma volume.

During this run of the HAARP-AGW experiment (6 August 2009 00:00-02:10 UTC), foF2 was approximately 3.9–4.0 MHz and the HAARP heater frequency was selected at  $f_{\text{HF}} = 3.3$  MHz (the highest value below 4 MHz allocated for the HAARP heater operation by the United States Federal Communications Commission). The digisonde was then configured to record F-region skymaps using sounding frequencies of 3.4–4.0 MHz in this case. The frequencies below 3.2 MHz were blocked by the daytime ionospheric E-layer, and frequencies too close to 3.3 MHz were saturated by the HAARP heater transmission at that time. Even though we were still able to discern some signatures of the generated AGW in the skymap data during this run, we need to remark that the above frequency configuration (where  $f_{\text{HF}} < f_{\text{SKYMAP}} < \text{foF2}$ ) was actually less than ideal. In general, a more optimum frequency configuration is one where  $f_{\text{SKYMAP}} < f_{\text{HF}} < \text{foF2}$ —provided that the local ionospheric plasma condition allows. We present below two additional cases of digisonde skymap observations under the latter (more optimum) frequency configuration.

Figure 4 shows a set of combined skymap echolocation data that we obtained from the HAARP-AGW experiment conducted on 19 July 2011 03:30-05:30 UTC. At that time, foF2 was approximately 5.2–5.3 MHz and the HAARP heater frequency was set at  $f_{\text{HF}} = 4.8$  MHz. During the experiment, skymaps were recorded once every minute using sounding frequencies of 2.8–4.2 MHz (in addition to one full ionogram taken every 5 min). The top panel of Fig. 4 is a color plot that depicts the zenith angle distribution of the skymap echoes as a function of time. Darker color corresponds to higher count of skymap echoes. Meanwhile, the bottom panel is a plot showing the *mode* (i.e. peak location) of this distribution histogram as a function of time. The purple markings on the time axis indicate the time period for this experiment, i.e. starting from 03:30 UTC ( $t = 210$  min) until 05:30 UTC ( $t = 330$  min).

From the zenith angle distribution-evolution plot shown on the top panel of Fig. 4, one can readily recognize the outward shifts in the skymap echolocation that occurred periodically according to the heater power modulation cycle. At their farthest extent, these outward streaks reached a maximum zenith angle of  $\sim 15^\circ$  away from vertical. In terms of linear coordinate distance, this radial progression corresponds to an outward shift of  $\sim 100$  km in  $\sim 10$  min. These observations suggest an apparent propagation speed of  $\sim 160$  m/s (along the horizontal direction) for the heater-generated artificial AGW/TID. Furthermore, we also note that the speed of the aforementioned outward shifts did not seem to correlate with the background  $\mathbf{E} \times \mathbf{B}$  plasma drift velocity that had been independently inferred during the time period of our experiment.

Finally, Fig. 5 depicts a few individual skymaps relevant to the HAARP-AGW experiment conducted on 25 October 2008 23:00-24:00 UTC. Prior to and during the experiment, F-region skymaps were recorded at an average rate of one skymap every 5 min. At that time period, foF2 was approximately 5.3–5.5 MHz and the HAARP heater frequency was set at  $f_{\text{HF}} = 4.5$  MHz. In the meantime, the digisonde used sounding frequencies of 3.9–4.5 MHz to record F-region skymaps. The top row of Fig. 5 shows a few skymaps taken from the time period before the HAARP-AGW heating started, whereas the bottom row shows a few sample skymaps recorded during the HAARP-AGW experiment. We indicate the instantaneous level of the transmitted HAARP power underneath each

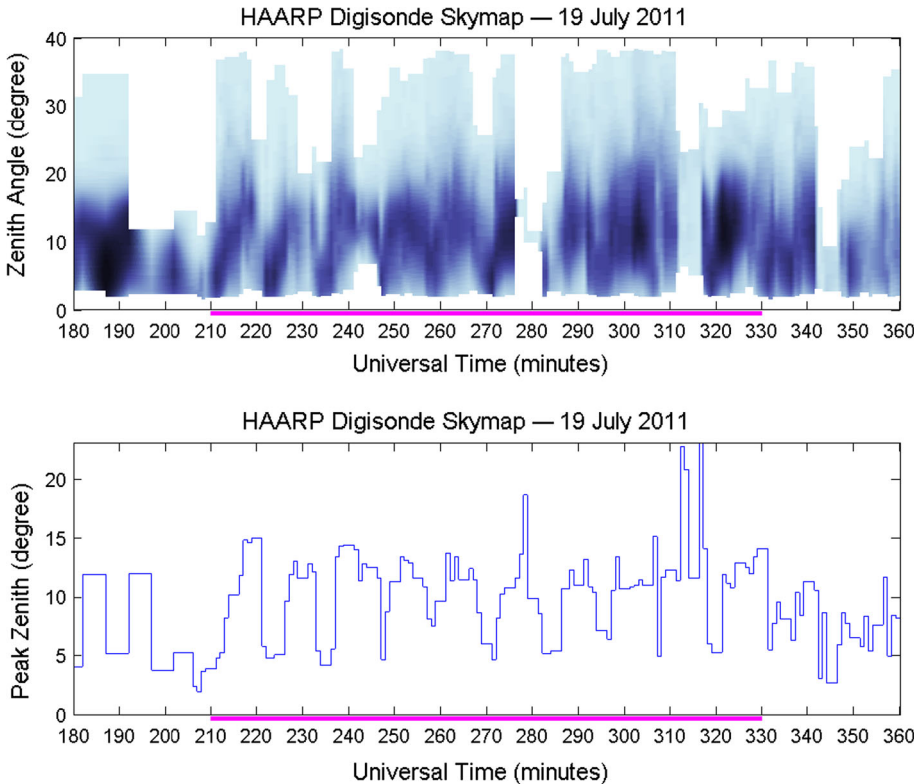


**Fig. 4** A set of combined digisonde skymap data from HAARP-AGW experiment on 19 July 2011 03:30–05:30 UTC. Time evolution of the zenith arrival angle distribution (*top*). The *mode* of the zenith arrival angle distribution as a function of time (*bottom*)

skymaps as well, along with an arrow sign representing the increasing/decreasing phase of the modulation cycle.

Before the experiment, the skymap echoes were distributed more-or-less uniformly in a cluster near the zenith/overhead direction (cf. top row of Fig. 5). On the other hand, during the HAARP-AGW experiment the skymap echo distribution changed periodically according to the heating modulation cycles and at times the return echoes also showed a characteristic pattern indicating some signatures of the artificial AGW/TID wavefronts (as seen in the sample skymaps listed on the bottom row of Fig. 5). In these skymaps-of-interest, the overall distribution of return echoes from the ionospheric F-region formed a concentric arc/ring around the HAARP-heated region. Such pattern is expected when artificial AGW/TID are being generated and propagate away from the heated region. The data from GPS TEC measurements during this run of the HAARP-AGW experiment are to be discussed in the next subsection.

### 3.3 GPS TEC Measurements

During the HAARP-AGW experiment on 25 October 2008 23:00–24:00 UTC, we had a scheduled pass of GPS satellite #30 near the HAARP facility. Throughout this GPS



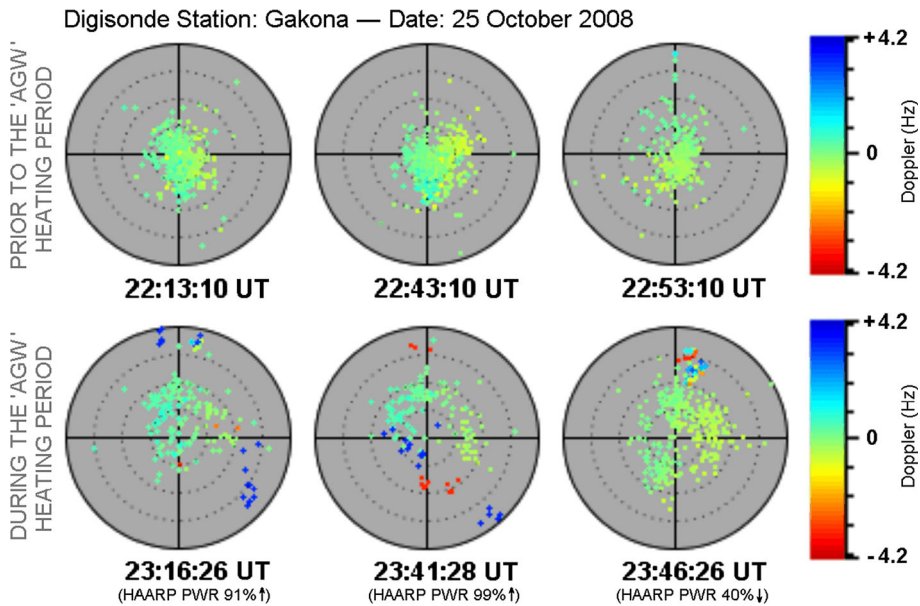


**Fig. 5** A set of digisonde sky map data recorded on 25 October 2008, showing a few individual snapshots of the F-region ionosphere prior to the HAARP-AGW experiment (*top row*) as well as those during the HAARP-AGW heating period (*bottom row*)

satellite pass, a receiver unit at the HAARP facility recorded essential information on the TEC along the connecting line between the receiver and the satellite. The measured TEC value was assigned to a specific point along this connecting line, i.e. the ionospheric piercing point (IPP), selected to be at 200 km altitude—near the foF2 peak. In this case, the IPP trajectory curved around and came relatively close to the heated region but did not actually enter/intersect the heated region. The point of closest approach happened at ~23:10 UTC; at this moment the IPP was turning around and started receding from the heated region. At the point of closest approach, the IPP was ~65 km away from the center of the heated region. We let the heater-generated artificial AGW/TID pass through the GPS IPP around the moment of closest approach, and then examined the TECP signal for characteristic patterns that would indicate the generation of AGW/TID from the heated region.

Figure 6 shows the results of the aforementioned GPS TEC measurements from the HAARP-AGW experiment on 25 October 2008. The top panel depicts the observed TECP signal during this GPS satellite pass. The purple line on the time axis (labeled “AGW Modulation”) marked the time period 23:00–24:00 UTC when we performed the heating modulation cycle. Next we examined the Fourier frequency spectra of this TECP signal, and we selected two separate time intervals for this purpose. The first time interval is 21:05–23:00 UTC ( $t = -175$  min to  $t = -60$  min), and it is used as a baseline. This interval is prior to the HAARP-AGW experiment. Meanwhile, the main time period of interest is 23:00–00:55 UTC ( $t = -60$  min to  $t = +55$  min). This interval is during/after the AGW modulation by the HAARP heater. Both time segments are of 115 min duration, and marked accordingly as blue intervals in the graph.

Even though the heating period in this run of the HAARP-AGW experiment was only 60 min in duration, it was actually necessary to use a longer time interval including the

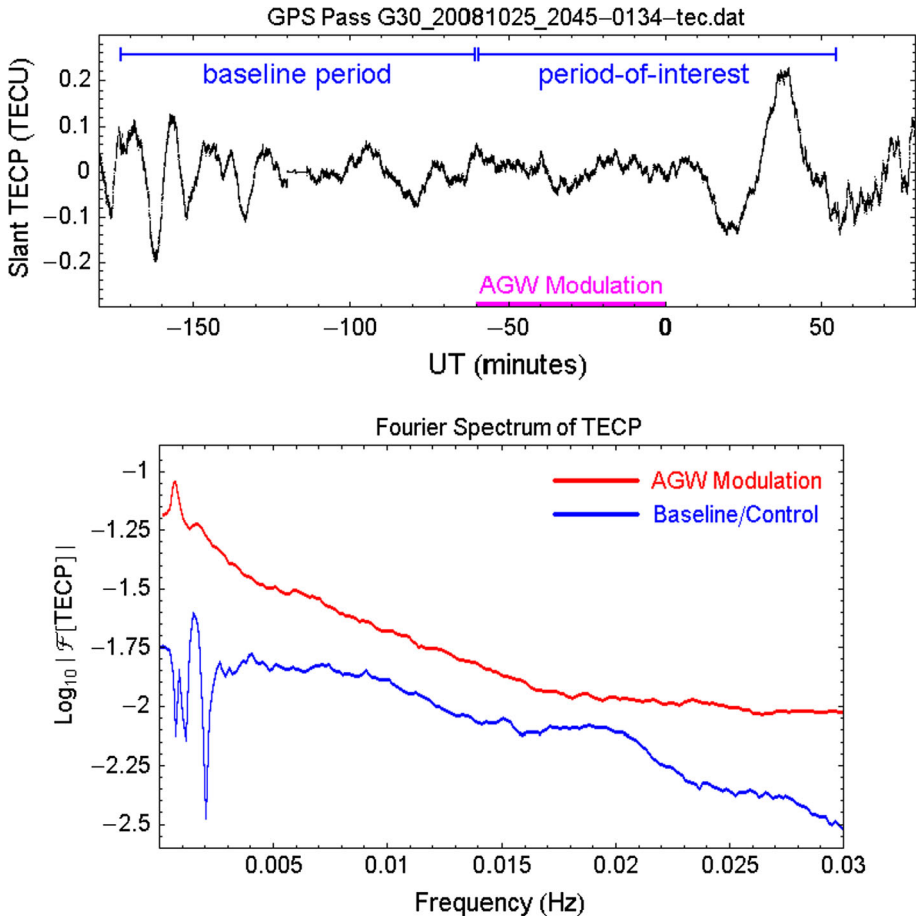


**Fig. 6** The results of our GPS TEC measurements for the HAARP-AGW experiment on 25 October 2008 23:00–24:00 UTC. The TECP signal during this GPS satellite pass (*top*). The Fourier frequency spectra of the TECP signal from time periods before and during/after the experiment (*bottom*)

time period after the heating had ended. During most of the HAARP-AGW heating period on 25 October 2008, the IPP of the GPS satellite was moving away from the heated region (the closest approach was at  $\sim 23:10$  UTC while the heating period started at 23:00 UTC). Here, we used a 115 min time interval (+55 min beyond the heating period) in order to allow for all of the outgoing AGW/TID wavefronts to catch up with the GPS IPP that had receded away. When the heating started at 23:00 UTC on 25 October 2008 ( $t = -60$  min), the GPS IPP was still closing in at a distance of  $\sim 69.7$  km from the center of the heated region. When the HAARP-AGW heating ended at 24:00 UTC ( $t = 0$  min), the GPS IPP had receded away to a distance of  $\sim 116$  km. At 00:55 UTC on 26 October 2008 ( $t = +55$  min), the GPS IPP was finally at a distance of  $\sim 292$  km away from the HAARP-heated region.

The bottom panel of Fig. 6 shows the Fourier spectra of the TECP signals from these two periods. The spectra from the time period of interest have a quite pronounced peak around 1 mHz, indicating a wavelike time variation in the TECP signal at this frequency—

as perceived in the IPP's rest frame. Note that we had modulated the transmitted HF heater power at a frequency of  $\sim 1.4$  mHz. During the time period of interest, the IPP was moving away from the heated region and therefore a redshift in the observed AGW frequency can be expected. The spectra from the baseline period, in relative comparison, looks rather flat at a much lower power level with some noisy fluctuation pattern in the 0–3 mHz frequency range.

#### 4 Discussion and Conclusion

The result of our experiments at the HAARP facility indicates that artificial AGW/TID can be generated in the ionosphere by the means of a modulated HF heating. In these experiments, the power envelope of the transmitted HF heater waves was sinusoidally varied in time with a period of  $2\pi/\Omega = 12$  min. This modulation period had been selected so that  $\Omega < \omega_g$ , where  $\omega_g$  is the local Brunt–Vaisala frequency at the interaction region. The data that came from a number of satellite and ground-based radio diagnostic instruments have given us positive indications that some artificial AGW/TID in fact emanated from the heated plasma volume during our experiments. The overall findings from 17 total runs of HAARP-AGW experiment over 5 years (2008–2012) have been consistent in general. The three separate runs discussed here are selected since the data were found to elucidate the characteristic signatures of the HAARP-induced artificial AGW/TID most clearly.

During the modulated heating, MUIR radar detected that the wind velocity outside the heated plasma volume was oscillating periodically with the same frequency as that of the heater power modulation cycle. The measurements had been carried out by tilting the MUIR radar beam  $15^\circ$  from vertical (away from the heated region), thereby letting any traveling plasma disturbances to pass through and then be intercepted by the narrow ( $\sim 3^\circ$ ) UHF radar beam.

Similar strategy was also used for our TEC measurements: as the GPS satellite's piercing point slowed down while turning around near (but still outside) the heated region, we let the traveling plasma disturbances pass through the LOS between the satellite and the on-site receiver. Analysis of these GPS measurements revealed a wavelike variation in the TECP signal for the time period during/after the modulated heating. This specific wavelike feature was not present during the control period just prior to the experiment.

Meanwhile, digisonde skymap measurements had allowed us to monitor a relatively large region inside the heated plasma volume and around it. In the skymap data recorded during the HAARP-AGW experiments, we observed a set of sequential outward shifts in the horizontal echolocations—closely following the 12-min heating modulation cycle. This special pattern suggests that we have some AGW/TID propagating out from the heated plasma volume. However, we would like also to point out a possible confounding factor associated with this skymap measurement as follows.

During heating, the heated region typically undergoes thermal expansion together with enhanced recombination along the magnetic flux tube (Lee et al. 1998), causing a slight bulge to form in the ionospheric plasma layer. This bulge acts like a “convex mirror” that makes the diagnostic HF wave rays from the digisonde to diverge when they reflect off the ionosphere overhead. The vertical-incidence rays would be more heavily affected, and one may therefore expect an overall reduction in the number of return echoes from around the zenith direction. This particular effect, when combined together with the actual characteristic signatures of heater-generated artificial AGW/TID, can be rather strenuous to disentangle. Furthermore, because of the general complexity in how HF ray trajectories can

change due to disturbances and/or turbulence in the ionosphere, there are potentially several other factors that might have contributed as well. An important approach to resolve this potential ambiguity is the use of multi-diagnostics, as we present in the current work. Several characteristic signatures of heater-generated artificial AGW/TID had been consistently observed via independent set of diagnostic techniques available at HAARP. Only radio diagnostic instruments have been employed so far, but some optical airglow diagnostics using our all sky imaging system are planned for future experiments.

In conclusion, we have carried out an experimental demonstration and theoretical analysis of AGW/TID generation process due to artificially-induced thermal gradients in ionospheric HF heating. By establishing the physical basis that thermal gradients may act as a source of free energy to generate some AGW/TID under controlled condition, we now have quite a firm ground to consider the possibility that the dynamical changes in large-scale natural thermal fronts (such as those appearing in heat wave events) could directly generate some AGW as well. Since powerful AGW could subsequently trigger some TID, we may thus expect that a severe and prolonged heat wave event could potentially induce widespread plasma turbulence in space. With the prospect that a warmer earth climate might lead to a more frequent occurrence of severe heat wave events (Meehl and Tebaldi 2004), it would be quite interesting for us to observe how the long-term pattern of AGW/TID in our ionosphere change statistically over time.

**Acknowledgments** The authors would like to thank James Secan from the Northwest Research Associate for providing GPS TEC data for our experiment on 25 October 2008. This work was supported by Air Force Office of Scientific Research (AFOSR) grant FA9550-09-1-0391 and High-frequency Active Auroral Research Program (HAARP) under Office of Naval Research (ONR) grant N00014-07-1-0999.

## References

- G.I. Grigor'ev, Moving ionospheric disturbances which develop during the operation of powerful transmitters. *Radiophys. Quantum Electron.* (English translation of *Izvestiya Vysshikh Uchebnykh Zavedenii, Radiofizika*) **18**(12), 1801–1805 (1975)
- V.E. Kunitsyn, E.S. Andreeva, V.L. Frolov, G.P. Komrakov, M.O. Nazarenko, A.M. Padokhin, Sounding of HF heating-induced artificial ionospheric disturbances by navigational satellite radio transmission. *Radio Sci.* **47**, RSOL15 (2012). doi:[10.1029/2011RS004957](https://doi.org/10.1029/2011RS004957)
- M.C. Lee, R.J. Riddolls, W.J. Burke, M.P. Sulzer, E.M.C. Klien, M.J. Rowlands, S.P. Kuo, Ionospheric plasma bubble generated by Arecibo heater. *Geophys. Res. Lett.* **25**, 579 (1998)
- J.G. Luhmann, Ionospheric disturbances resulting from ion-neutral coupling. *Space Sci. Rev.* **34**, 337–346 (1983)
- G.A. Meehl, C. Tebaldi, More intense, more frequent, and longer lasting heat waves in the 21st century. *Science* **305**, 994 (2004). doi:[10.1126/science.1098704](https://doi.org/10.1126/science.1098704)
- E. Mishin, E. Sutton, G. Milikh, I. Galkin, C. Roth, M. Forster, F2-region atmospheric gravity waves due to high-power HF heating and subauroral polarization streams. *Geophys. Res. Lett.* **39**, L11101 (2012). doi:[10.1029/2012GL052004](https://doi.org/10.1029/2012GL052004)
- NOAA Documentation, Evidence for precipitation of energetic particles by ionospheric heating transmissions, National Geophysical Data Center (2004), <http://www.ngdc.noaa.gov/stp/IONO/Dynasonde/SpEatHeating.htm>
- R. Pradipta, Could global warming affect space weather? Case studies of intense ionospheric plasma turbulence associated with natural heat source, MS thesis, MIT (2007)
- R. Pradipta, Generation of acoustic-gravity waves in ionospheric HF heating experiments: simulating large-scale natural heat sources, Ph.D. Dissertation, MIT (2012)
- J.W. Wright, Evidence for precipitation of energetic particles by ionospheric heating transmissions. *J. Geophys. Res.* **80**, 31 (1975)